Synthesis of nutrient and sediment export patterns in the Chesapeake Bay watershed: Complex and non-stationary concentration-discharge relationships

Qian Zhang [a, b, *]

[a] University of Maryland Center for Environmental Science / U.S. Environmental Protection Agency Chesapeake Bay Program, 410 Severn Avenue, Suite 112, Annapolis, MD 21403, USA

[b] Formerly, Johns Hopkins University, Department of Geography and Environmental Engineering, 3400 North Charles Street, Ames Hall 313, Baltimore, MD 21218, USA

[*] *Corresponding author*. Tel.: +1-443-509-2270; E-mail address: qzhang@chesapeakebay.net.

Abstract

Derived from river monitoring data, concentration-discharge (*C*-*Q*) relationships are useful indicators of riverine export dynamics. A top-down synthesis of *C*-*Q* patterns is provided for suspended sediment (SS), total phosphorus (TP), and total nitrogen (TN) for nine major tributaries (15 sites) to Chesapeake Bay, which represent diverse characteristics in terms of land use, physiography, and hydrological settings. Model coefficients from the recently-developed WRTDS (Weighted Regressions on Time, Discharge, and Season) method were used to make informative interpretation of *C*-*Q* relationships. Unlike many previous *C*-*Q* studies that focused on stormflow conditions, this approach allows simultaneous examination of various discharge conditions within an uncertainty framework. This synthesis on WRTDS coefficients (*i.e.*, the sensitivity of concentration to discharge) has offered new insights on the complexity of watershed function. Results show that watershed export has been dominated by mobilization patterns for SS and TP (particulate-dominated species) and chemostasis patterns for TN (dissolved-dominated species) under many discharge conditions. Among nine possible modalities of low-flow *vs*. high-flow patterns, the three most frequent modalities are mobilization-mobilization (17 cases), chemostasis-mobilization (13 cases), and chemostasis-chemostasis (7 cases), representing 82% of all 45 watershed-constituent pairs. The general lack of dilution patterns may suggest that none of these constituents has been supply-limited in these watersheds. For many site-constituent combinations, results show clear temporal non-stationarity in *C*-*Q* relationships under selected time-invariant discharges, reflecting major changes in dominant watershed sources due to anthropogenic actions. These results highlight the potential pitfalls of assuming fixed *C*-*Q* relationships in the record. Overall, this work demonstrates the utility of WRTDS model coefficients for interpretation of river water-quality data and for generation of sensible hypotheses on dominant processes in different watersheds. The approach is readily adaptable to other river systems, where long-term discretely-sampled data are available, to decipher complex interactions between hydrological and biogeochemical processes.

Keywords

C-Q relationship, watershed function, watershed sources, management, stationarity, WRTDS.

1. Introduction

Derived from river monitoring data, concentration-discharge (*C*-*Q*) relationships are a powerful tool for understanding complex interactions between hydrological and biogeochemical processes, including solute and particulate export dynamics (Evans and Davies, 1998; Chanat *et al.*, 2002; Godsey *et al.*, 2009; Thompson *et al.*, 2011; Meybeck and Moatar, 2012; Musolff *et al.*, 2015; Moatar *et al.*, 2017). In particular, *C*-*Q* relationships have been commonly classified into three categories – namely, "dilution" *(i.e.*, negative relationship); "mobilization" (*i.e.*, positive relationship); and "chemostasis" (*i.e., C* invariant with *Q*). Such classifications have been found to vary with constituent and with site (Godsey *et al.*, 2009; Hirsch *et al.*, 2010; Meybeck and Moatar, 2012; Stallard and Murphy, 2014; Herndon *et al.*, 2015; Musolff *et al.*, 2015; Moatar *et al.*, 2017).

In general, *C*-*Q* relationships are largely controlled by the spatial availability and distribution of constituent sources in the various compartments as well as their hydrological connectivity to the stream channel. Particularly, dilution responses can occur when anthropogenic point sources (*e.g.*, wastewater treatment plants) or other spatially distinct and flow-independent sources (*e.g.*, mineral dissolution from base-flow pathways) are dominant and are more concentrated than nonpoint sources in the watershed. Mobilization responses can occur when otherwise disconnected solute or sediment sources become connected to water flow paths during elevated discharges. Mobilization and dilution are often described as transport- and source- limitation, respectively. These conceptualizations have formed the foundation to the development of component mixing models for interpretation of event-scale concentration data in terms of contributions from deep subsurface, shallow subsurface, and surface water sources (Evans and Davies, 1998; Chanat *et al.*, 2002; Bieroza and Heathwaite, 2015) and riverine loading apportionment models for analysis of decadal-scale records (Bowes *et al.*, 2008; Bowes *et al.*, 2009). As a relatively less familiar concept, chemostasis has been recently documented for nutrients and weathering products in a range of watersheds and has been attributed to constant fluxes of release from legacy stores that have been accumulated historically from sources such as agricultural input, atmospheric deposition, and mineral formation and deposition (Godsey *et al.*, 2009; Basu *et al.*, 2010; Basu *et al.*, 2011; Thompson *et al.*, 2011; Herndon *et al.*, 2015).

While many prior *C-Q* studies focused on the interpretation of event-scale data (*e.g.*, storm hysteresis) and the development of component mixing models for inferring source water (Evans and Davies, 1998; House and Warwick, 1998; Outram *et al.*, 2014; Bieroza and Heathwaite, 2015), decadal-scale discretely-sampled (low-frequency) data also have merits. In particular, such long-term data can reveal temporal changes in *C-Q* relationships, which in turn may reflect long-term shifts in watershed function due to anthropogenic activities such as land disturbance and watershed management (Bieroza and Heathwaite, 2015; Burt *et al.*, 2015; Gray *et al.*, 2015; Zhang *et al.*, 2016d; Moatar *et al.*, 2017). In this regard, several recent *C-Q* studies focused on "top-down" synthesis of long-term data from multiple watersheds with the common feature of searching for parsimonious representation of dominant watershed processes (Godsey *et al.*, 2009; Basu *et al.*, 2010; Thompson *et al.*, 2011).

While the adoption of log-linear *C-Q* relationship (or its modified form, log-linear loading-discharge relationship) has been a popular practice in the hydrological literature, there are several issues noted with this approach that can complicate or even mislead the interpretation. These issues include non-linear *log(C)-log(Q)* relations and variations in relation over time and season due to changes in constituent availability and biochemical modulation. Zhang *et al.* (2016c) discussed these issues with real-world examples and proposed an improved approach that uses the model coefficients from the recently-developed WRTDS ("Weighted Regressions on Time, Discharge, and Season") method (Hirsch *et al.*, 2010) to provide informative interpretation of *C-Q* patterns in long-term, discretely-sampled data.

This work builds upon the work of Zhang *et al.* (2016c) to better understand constituent export patterns from the multi-jurisdictional watershed of Chesapeake Bay, the largest estuary in the North America. For this watershed, reduction of total nitrogen (TN), total phosphorus (TP), and suspended sediment (SS) loads has long been a management focus toward controlling Bay eutrophication and hypoxia (Kemp *et al.*, 2005; Murphy *et al.*, 2011; Shenk and Linker, 2013). For assessment of past management progress and development of future restoration strategies, it is critical to understand export from different areas of the watershed. In this context, the main objective of this work was to apply the approach of Zhang *et al.* (2016c) to long-term (~ 30 years) data covering three major constituents (*i.e.*, SS, TP, and TN) for nine major tributaries to Chesapeake Bay (**Fig. 1**). This work is presumably the first top-down analysis of *C-Q* patterns in the Chesapeake Bay watershed, which was aimed to address two research questions:

(1) How does the prevalence of *C*-*Q* relationship vary by discharge condition and how does the pattern compare among sites and species?

(2) How does *C*-*Q* relationship vary over time under different discharge conditions and how does the pattern compare among sites and species?

These questions have been similarly explored by Moatar *et al.* (2017) in a number of French watersheds using a "split-hydrograph" method, where *C*-*Q* relationship is separately modeled for below- and above- median discharge conditions. In comparison, the approach proposed by Zhang *et al.* (2016c) provides a more flexible and comprehensive representation of the *C*-*Q* relationship across discharge, temporal, and seasonal conditions, and it has the capability of dealing with censored (below detection limit) concentrations.

2. Methods

2.1. Monitoring Sites

This work focused on nine major tributaries to Chesapeake Bay, namely, Susquehanna, Potomac, James, Rappahannock, Appomattox, Pamunkey, Mattaponi, Patuxent, and Choptank, which represent diverse characteristics in terms of land use, physiography, and hydrological settings (**Fig. 1; Table 1**). Since the 1980s, these rivers have been monitored at their fall-line locations (divide of tidal and non-tidal areas) by the U.S. Geological Survey (USGS) River Input Monitoring (RIM) Program. Collectively, these sites account for ~93% of non-tidal discharge and ~77% of total freshwater discharge to Chesapeake Bay between 1991 and 2000 (Shenk and Linker, 2013). The Choptank is located entirely in the coastal plain and may represent the much larger Eastern Shore. On the Western Shore, only Mattaponi draws a substantial portion of its water from the coastal plain. The other tributaries are dominated by upland physiographic provinces, including piedmont, Blue Ridge, valley and ridge, and Appalachian plateau (Shenk and Linker, 2013).

In terms of export from the nine tributaries, Susquehanna contributed ~62% of river discharge , ~65% of TN load, ~46% of TP load, and ~41% of SS load between 1979 and 2012 (Zhang *et al.*, 2015). The relatively lower fractional contributions of TP and SS reflect historical retention within the Lower Susquehanna River Reservoir System (LSRRS). The most-downstream member of the LSRRS, Conowingo Reservoir, is reportedly over 90% full in terms of sediment storage (Langland, 2015), accompanied by substantial recent decline in net trapping of sediment and particulate nutrients (Hirsch, 2012; Zhang *et al.*, 2013; Zhang *et al.*, 2016d). Below the LSRRS, one site has been managed by the USGS, which is the RIM site at Conowingo Dam, Maryland. Above the LSRRS, six sites have been monitored by the Susquehanna River Basin Commission (SRBC) since the 1980s, with three of them (*i.e.*, Towanda, Danville, and Marietta) on the main-stem of Susquehanna and the other three (*i.e.*, Lewisburg, Newport, and Conestoga) on tributaries to Susquehanna (**Fig. 1; Table 1**).

2.2. Monitoring Data

For each site, daily discharge data were compiled from the USGS National Water Information System (NWIS) (U.S. Geological Survey, 2014). In addition, SS, TP, and TN concentration data were compiled from NWIS for the nine RIM sites (U.S. Geological Survey, 2014) and from SRBC for the six Susquehanna sites above LSRRS (Susquehanna River Basin Commission, 2014). These sites are among the most densely sampled long-term stations within the Chesapeake Bay Nontidal Water-Quality Monitoring Network (Chanat *et al.*, 2016). The average number of days sampled varies with sites, ranging between 12.6–39.4 days/year (median = 25.7) for SS, 20.8–40.4 days/year (median = 28.3) for TP, and 20.8–39.4 days/year (median = 27.6) for TN. See **Table 2** for details of data coverage.

In general, water-quality concentration samples at each site were collected across the full range of hydrologic conditions in each year and comprised of at least eight targeted stormflow samples and twelve regular samples (Chanat *et al.*, 2016; Zhang *et al.*, 2016a). Consequently, these sites have been sampled at least 20 days per year (**Table 2**). The only exceptions are SS records at one RIM site in Maryland (Potomac) and all five RIM sites in Virginia. To coarsely examine the representativeness of water-quality sampling with respect to flow conditions, distributions of discharge on days with water-quality samples and discharge on all days in the record were compared. Results show that SS, TP, and TN have been sampled with generally good coverage of high-flow conditions – see **Fig. S1-S3** in the online supplementary material.

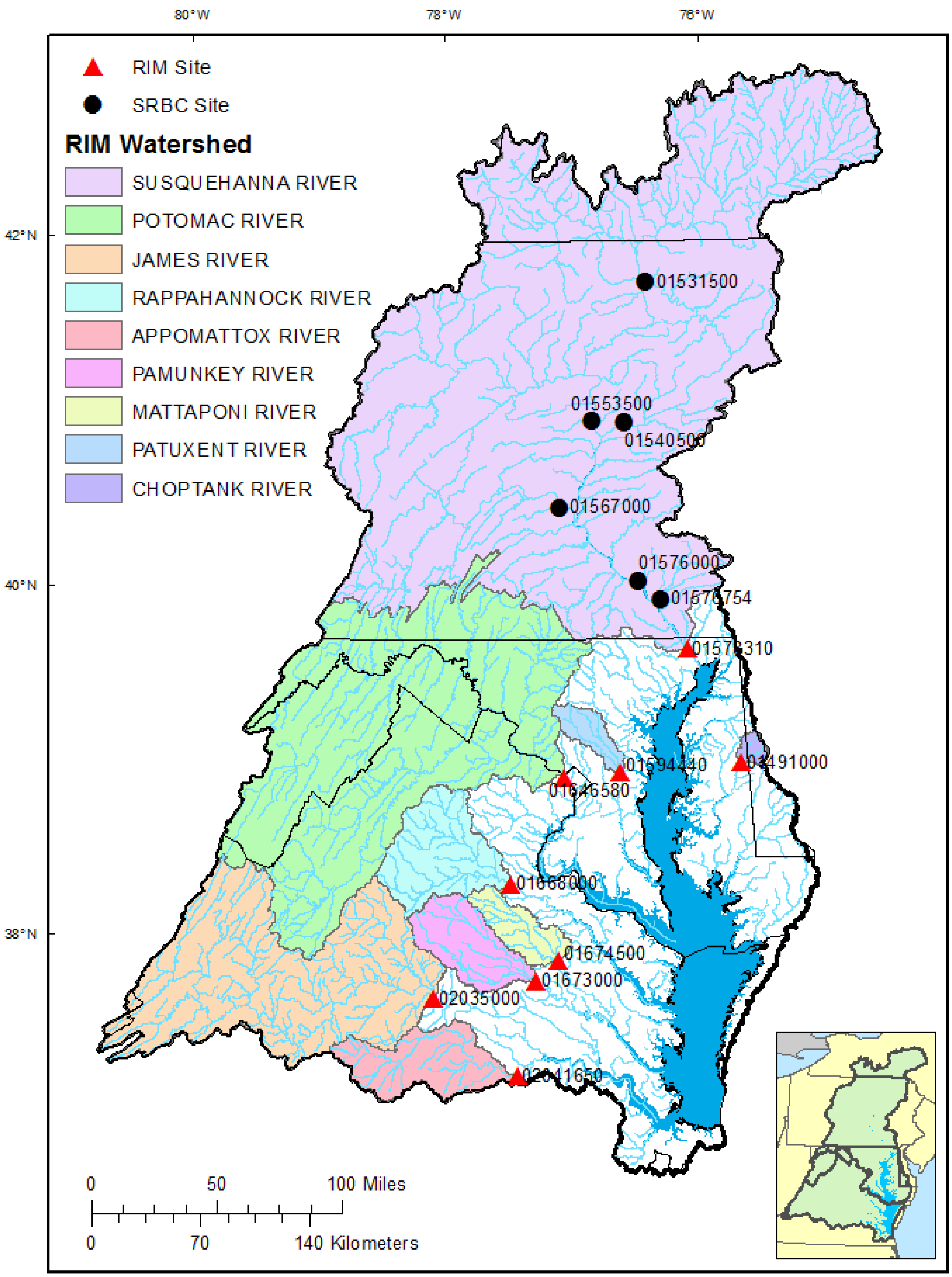

BASE FROM U.S. GEOLOGICAL SURVEY 1:2,000,000
STATE BOUNDARY DIGITAL LINE GRAPH,
ALBERS EQUAL AREA PROJECTION, NAD 1983

Fig. 1. Chesapeake Bay watershed and the 15 monitoring sites that include nine River Input Monitoring (RIM) sites on the fall-line of nine major tributaries and six Susquehanna River Basin Commission (SRBC) sites at upstream locations within the Susquehanna River basin.

Table 1. Details of the 15 long-term monitoring sites in the Chesapeake Bay watershed. [a]

	Station Number	River sites	Drainage area, km^2	Annual river flow in 1984-2014		Upstream land use (percent)			
				Average flow, m^3/s	Average yield, m/yr	Urban	Agricultural	Forested	Other
RIM Sites	01578310	Susquehanna River near Conowingo, MD	70,189	1147	0.52	2	29	67	2
	01646580	Potomac River at Chain Bridge, Washington D.C.	30,044	338	0.35	3	35	61	1
	02035000	James River at Cartersville, VA	16,213	199	0.39	1	16	80	3
	01668000	Rappahannock River near Fredericksburg, VA	4,144	49	0.38	1	36	61	2
	02041650	Appomattox River at Matoaca, VA	3,471	33	0.30	1	20	72	7
	01673000	Pamunkey River near Hanover, VA	2,800	28	0.31	1	24	68	7
	01674500	Mattaponi near Beulahville, VA	1,557	15	0.30	1	19	69	11
	01594440	Patuxent River at Bowie, MD	901	11	0.38	13	41	38	8
	01491000	Choptank River near Greensboro, MD	293	4.2	0.45	1	50	29	20
SRBC Sites	01576000	Susquehanna River at Marietta, PA	67,314	1114	0.52	4	30	64	2
	01540500	Susquehanna River at Danville, PA	29,008	475	0.52	5	33	60	2
	01531500	Susquehanna River at Towanda, PA	20,194	325	0.51	4	35	60	1
	01553500	West Branch Susquehanna River at Lewisburg, PA	17,765	310	0.55	2	15	81	2
	01567000	Juniata River at Newport, PA	8,687	126	0.46	2	28	69	1
	01576754	Conestoga River at Conestoga, PA	1,217	19	0.50	8	54	37	1

[a] modified from Table 3 and Table 8 in Sprague *et al.* (2000)

Table 2. Temporal coverage of observed water-quality data at the 15 Chesapeake sites.
(T_{start}: first sampled day; T_{end}: last sampled day; N_{sample}: total number of sampled days; f_{sample}: average number of sampled days per year.)

	River sites	Suspended Sediment (SS)			Total Phosphorus (TP)			Total Nitrogen (TN)		
		T_{start}	T_{end}	N_{sample} (f_{sample})	T_{start}	T_{end}	N_{sample} (f_{sample})	T_{start}	T_{end}	N_{sample} (f_{sample})
USGS RIM Sites	Susquehanna River near Conowingo, MD	1984/10/25	2014/9/3	799 (26.6/yr)	1984/10/25	2014/9/3	808 (26.9/yr)	1984/10/25	2014/9/3	804 (26.8/yr)
	Potomac River at Chain Bridge, Washington D.C.	1984/11/14	2014/9/9	463 (15.4/yr)	1984/10/9	2014/9/9	1191 (39.7/yr)	1984/10/2	2014/9/9	1183 (39.4/yr)
	James River at Cartersville, VA	1984/10/30	2014/9/2	475 (15.8/yr)	1984/10/30	2014/9/2	814 (27.1/yr)	1984/10/30	2014/9/2	811 (27.0/yr)
	Rappahannock River near Fredericksburg, VA	1984/10/9	2014/9/9	381 (12.7/yr)	1984/10/9	2014/9/9	763 (25.4/yr)	1984/10/9	2014/9/9	756 (25.2/yr)
	Appomattox River at Matoaca, VA	1984/11/20	2014/9/4	385 (12.8/yr)	1984/11/20	2014/9/4	779 (26.0/yr)	1984/11/20	2014/9/4	773 (25.8/yr)
	Pamunkey River near Hanover, VA	1984/10/17	2014/9/16	386 (12.9/yr)	1984/10/17	2014/9/16	831 (27.7/yr)	1984/10/17	2014/9/16	828 (27.6/yr)
	Mattaponi near Beulahville, VA	1984/10/17	2014/9/30	378 (12.6/yr)	1984/10/17	2014/9/30	819 (27.3/yr)	1984/10/17	2014/9/30	813 (27.1/yr)
	Patuxent River at Bowie, MD	1984/11/28	2014/9/26	771 (25.7/yr)	1984/10/24	2014/9/26	849 (28.3/yr)	1984/10/24	2014/9/26	771 (25.7/yr)
	Choptank River near Greensboro, MD	1984/10/19	2014/9/25	613 (20.4/yr)	1984/10/19	2014/9/25	625 (20.8/yr)	1984/10/19	2014/9/25	624 (20.8/yr)
SRBC Sites	Susquehanna River at Marietta, PA	1986/10/7	2014/9/29	1037 (37.0/yr)	1986/10/7	2014/9/29	1044 (37.3/yr)	1986/10/7	2014/9/29	1043 (37.3/yr)
	Susquehanna River at Danville, PA	1984/10/11	2014/9/30	1183 (39.4/yr)	1984/10/11	2014/9/30	1213 (40.4/yr)	1984/10/11	2014/9/30	1082 (36.1/yr)
	Susquehanna River at Towanda, PA	1988/10/5	2014/9/15	990 (38.0/yr)	1984/10/10	2014/9/15	1061 (35.4/yr)	1984/10/10	2014/9/15	931 (31.0/yr)
	West Branch Susquehanna River at Lewisburg, PA	1984/10/11	2014/9/30	1130 (37.7/yr)	1984/10/11	2014/9/30	1165 (38.8/yr)	1984/10/11	2014/9/30	1031 (34.4/yr)
	Juniata River at Newport, PA	1984/10/10	2014/9/17	1006 (33.5/yr)	1984/10/10	2014/9/17	1050 (35.0/yr)	1984/10/10	2014/9/17	914 (30.5/yr)
	Conestoga River at Conestoga, PA	1984/10/18	2014/9/29	1076 (35.9/yr)	1984/10/18	2014/9/29	1065 (35.5/yr)	1984/10/18	2014/9/29	1014 (33.8/yr)

2.3. Statistical Method

WRTDS estimates daily constituent concentrations and loadings based on discretely-sampled concentration data (Hirsch *et al.*, 2010):

$$ln(C_i) = \beta_{0,i} + \beta_{1,i}t_i + \beta_{2,i}\, ln(Q_i) + \beta_{3,i}\, sin(2\pi t_i) + \beta_{4,i}\, cos(2\pi t_i) + \varepsilon_i \quad (1)$$

where t_i is time in decimal years, C_i is daily concentration at time t_i, Q_i is daily discharge at time t_i, $\beta_{0,i}$ ~ $\beta_{4,i}$ are fitted coefficients, and ε_i is the error term. For each estimation day, WRTDS pre-screens all available samples and selects the most relevant samples to fit Equation (1), with the "relevancy" being quantified on three dimensions, *i.e.*, time, discharge, and season. The fitted coefficients are used to estimate $ln(C_i)$ on the estimation day with known values of t_i and Q_i. To expedite estimation, WRTDS establishes a set of evenly-spaced grid points on a surface defined by t and $ln(Q)$, develops individual model for each grid point, and performs bi-linear interpolations among the grid points to generate a surface of concentration estimates (*i.e.*, C as functions of t and Q). The estimation process is fully described in Hirsch and De Cicco (2015).

For interpretation of C-Q relationships, Zhang *et al.* (2016c) recommended use of WRTDS β_2 coefficients over traditional approaches. Specifically,

(1) It does not assume a linear $ln(C)$~$ln(Q)$ relation.
(2) It allows the C-Q relation to flexibly vary with time, discharge, and season.
(3) It conducts local fitting at many points in the t-Q space in a consistent manner.
(4) It can decouple the interactions among time, discharge, and season.
(5) It is less sensitive than other approaches to the scarcity of highflow samples.
(6) It can deal with concentration data set that contains censored values.

2.4. Data Analyses

For each constituent and each site, WRTDS was implemented using the *EGRET* (Exploration and Graphics for RivEr Trends) package version 2.2.0 (Hirsch and De Cicco, 2015) in R 3.1.0 (R Development Core Team, 2014). *R* codes published by Zhang *et al.* (2016c) and documented at the Johns Hopkins University Data Archive (Zhang *et al.*, 2016b) were applied to estimate, extract, and visualize the β_2 coefficients. In addition, variance inflation factor (Kutner *et al.*, 2004) was calculated for each regression to confirm that collinearity among the independent variables was not an issue.

WRTDS β_2 coefficients are used to categorize export patterns – namely, (1) "dilution" *(i.e.,* $\beta_2 < 0$); (2) "chemostasis" ($\beta_2 \approx 0$); and (3) "mobilization" ($\beta_2 > 0$). Following prior investigations (Godsey *et al.*, 2009; Herndon *et al.*, 2015), the range of -0.1 to 0.1 is considered as chemostasis. For illustration, the estimated β_2 coefficients for TP in Susquehanna River at Conowingo are shown as a contour plot against axes of t and $ln(Q)$ in **Fig. 2**.

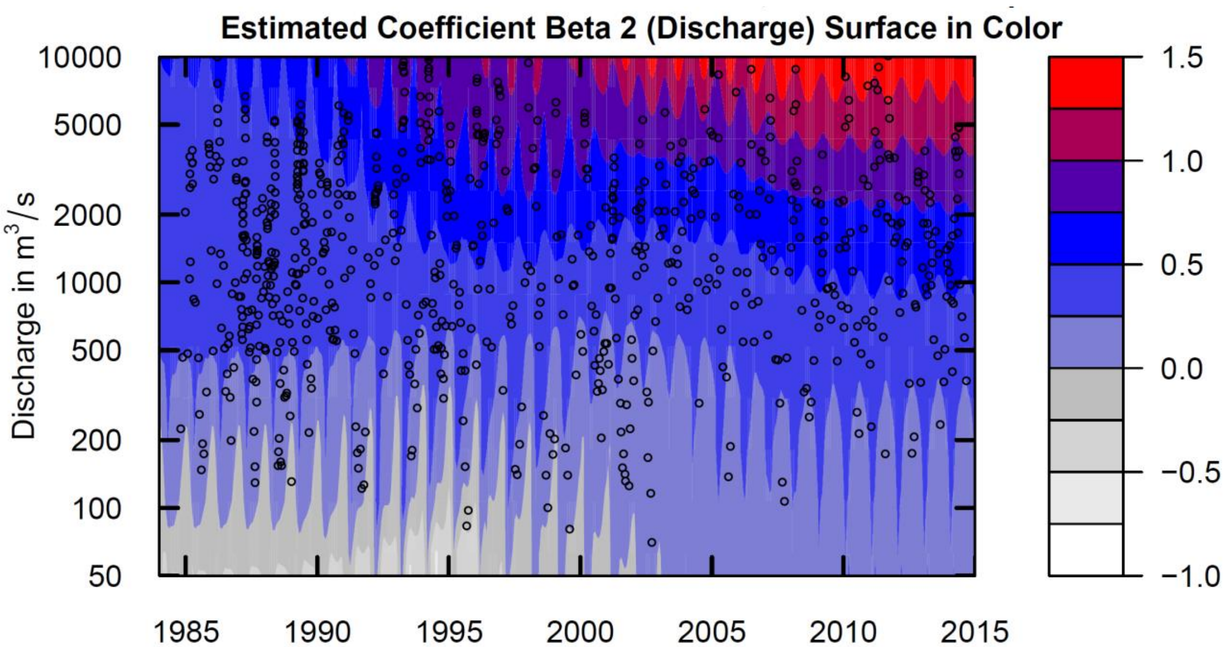

Fig. 2. Contour plot showing estimated WRTDS β_2 coefficients as a function of time and discharge for total phosphorus in Susquehanna River at Conowingo, MD. Black open circles indicate the time-discharge combinations where concentration samples have been taken. The β_2 coefficients correspond to three broad categories, namely, (1) dilution *(i.e.,* $\beta_2 < 0$); (2) chemostasis ($\beta_2 \approx 0$); and (3) mobilization ($\beta_2 > 0$).

To address the first question posited above, daily β_2 coefficients were grouped by discharge percentiles to reveal discharge-related patterns for each site-constituent pair. These results are presented in **Section 3.1** (**Fig. 3-5**) and discussed in **Section 4.1**. To address the second question, β_2 coefficients were grouped by year under three selected discharge conditions to accommodate the effects of inter-annual discharge variability. Because β_2 coefficients were estimated for 14 fixed discharge levels, the discharges closest to the 10^{th}, 60^{th}, and 99.5^{th} percentiles of the site-specific daily discharge distribution were used to represent low-, mid-, and high- discharge conditions, respectively. For each discharge, β_2 coefficients were extracted and their annual averages were calculated. These results are presented in **Section 3.2** (**Fig. 6-8**) and discussed in **Section 4.2**. Following Zhang *et al.* (2016c), 90% confidence intervals were quantified for these annual averages using the block-bootstrap method of Hirsch *et al.* (2015), which resamples (with replacement) the original concentration data to obtain 50 realizations of representative sets and re-run the model estimation with each replicate. The period-of-record change in annual β_2 coefficient (Δ) was quantified, *i.e.*, $\Delta = \beta_{2, yr\ 2014} - \beta_{2, yr\ 1984}$. The probability of positive change ("$P_{\Delta>0}$") or negative change ("$P_{\Delta<0}$") was calculated for the 50 bootstrap runs for each site-constituent pair (**Table 4**).

3. Results

3.1. Changes in *C-Q* Pattern over Discharge

SS coefficients show predominantly mobilization effects across all discharge intervals at the 15 Chesapeake sites (**Fig. 3**). Exceptions include five sites at the lowest discharge interval (Towanda, Conowingo, Rappahannock, Appomattox, and Mattaponi) and one site at the highest discharge interval (Mattaponi). For such exceptions, median coefficient is close to zero, indicating chemostasis or even dilution. At most sites, SS coefficients follow a positive monotonic pattern with respect to discharge, with the highest values occurring at the highest discharge interval (*i.e.*, 90^{th}~100^{th} percentile). Deviations from this general pattern are observed in several cases. For the low-discharge intervals, coefficients are not correlated with discharge at two sites (Pamunkey and Choptank). For the high-discharge intervals, coefficients appear to level off at three sites (Marietta, Appomattox, and Choptank) and decrease with discharge at six sites (Potomac, James, Rappahannock, Pamunkey, Mattaponi, and Patuxent).

TP coefficients also show predominantly mobilization patterns at many discharge intervals, but TP coefficients are generally smaller than SS coefficients (**Fig. 4**). Exceptions (*i.e.*, chemostasis or dilution) are observed with all sites at the lowest discharge and two sites at the highest discharge (Pamunkey and Mattaponi). In terms of relationship with discharge, TP coefficients generally follow a positive monotonic pattern. Deviations from this pattern are observed: for the low-discharge intervals, coefficients are not correlated with discharge at four sites (Newport, Appomattox, Pamunkey and Choptank); for the high-discharge intervals, coefficients decline with discharge at five sites (Rappahannock, Pamunkey, Mattaponi, Patuxent, and Choptank).

TN coefficients show patterns that are very different from SS or TP: mobilization effect is not dominant; instead, chemostasis or nearly-chemostatic effects are much more prevalent for many discharge intervals (**Fig. 5**). In addition, TN coefficients are generally smaller than SS and TP coefficients. Several exceptions (*i.e.*, non-chemostatic effects) are observed, including mobilization at Newport, Potomac, James, and Rappahannock for most discharge intervals as well as dilution at Conestoga for high-discharge intervals and Patuxent for all discharge intervals. In terms of relationship with discharge, TN coefficients show monotonic decline with discharge at three sites (Newport, Conestoga, and Potomac), monotonic increase with discharge at two sites (James and Appomattox), but no correlation with discharge at all other sites.

These results (**Fig. 3-5**) show strong contrast between low-flow and high-flow *C-Q* patterns. As a more focused analysis, such contrast is summarized for the lowest and highest discharge intervals, *i.e.*, $Q_{0\text{-}10th}$ *vs*. $Q_{90\text{-}100th}$, in **Table 3**, where mobilization, chemostasis, and dilution are indexed as M, C, and D, respectively. Theoretically, there are nine possible modalities, namely, M-M, M-C, M-D, C-M, C-C, C-D, D-M, D-C, and D-D. For SS, only two modalities exist, which are M-M (10 sites) and C-M (5 sites). In other words, dilution is always absent and mobilization is always the pattern at the highest discharge interval. For TP, four modalities exist, namely, C-M (7 sites), M-M (4 sites), D-M (3 sites), and C-C (1 site). TP is also dominated by mobilization at the highest discharge but TP behaves more diversely than SS at the lowest discharge. For TN, six modalities exist, which are more diverse than SS and TP. The most frequent modalities are C-C (6 sites), M-M (3 sites), and M-C (3 sites), all irrelevant to dilution. Considering all three constituents at the 15 sites (45 cases), the most frequent modalities are M-M (17 cases), C-M (13 cases), and C-C (7 cases), which represent 82% of all cases.

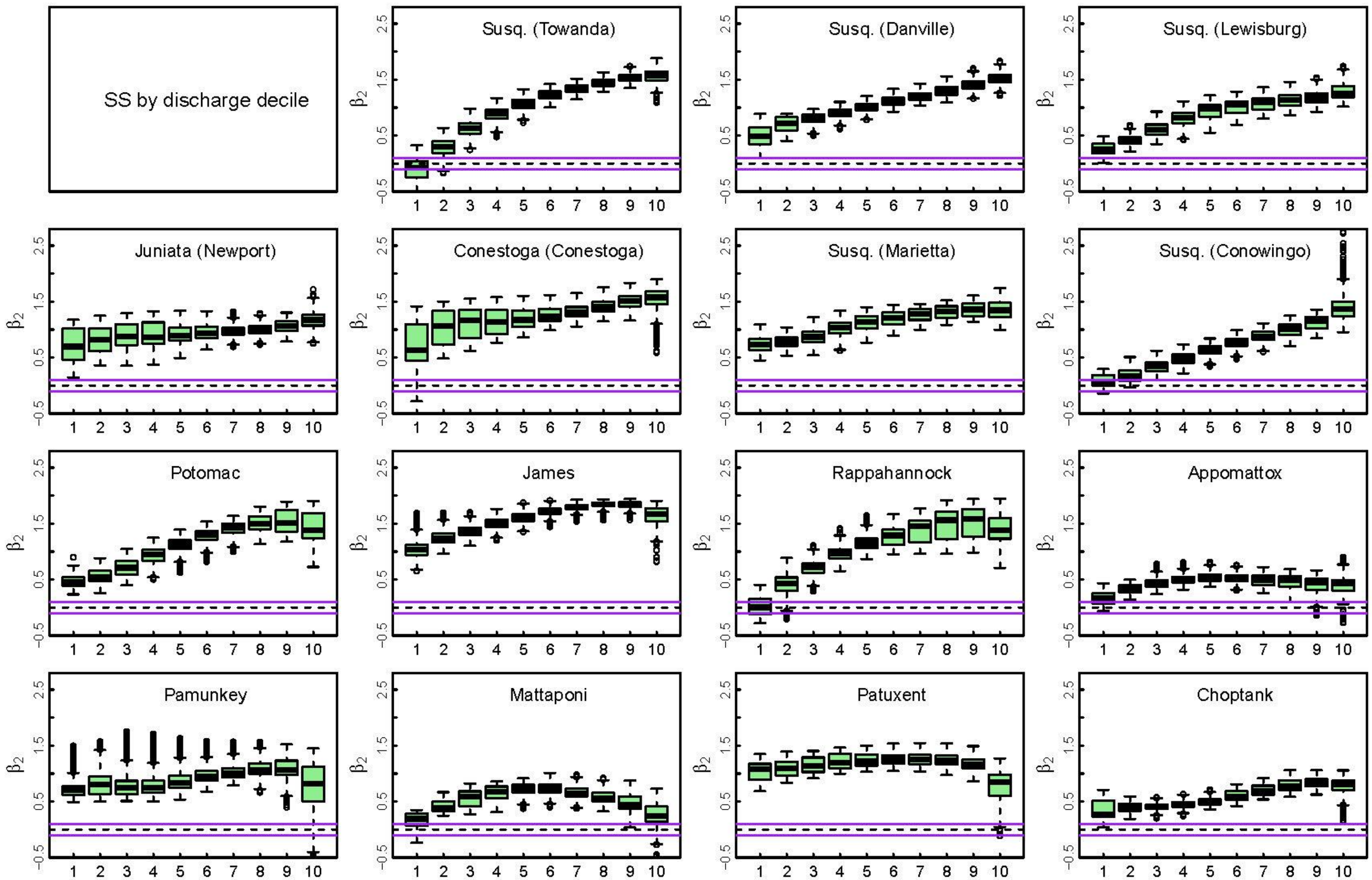

Fig. 3. Boxplot summary of estimated WRTDS β_2 coefficients by discharge decile for suspended sediment (SS) at the 15 Chesapeake sites. X-axis shows flow bins: 1 = 0^{th}~10^{th}, 2 = 10^{th}~20^{th}…, 9 = 80^{th}~90^{th}, 10 = 90^{th}~100^{th}. The region between the purple horizontal lines (*i.e.*, between -0.1 and 0.1) represents chemostasis. Regions above and below it represent mobilization and dilution, respectively.

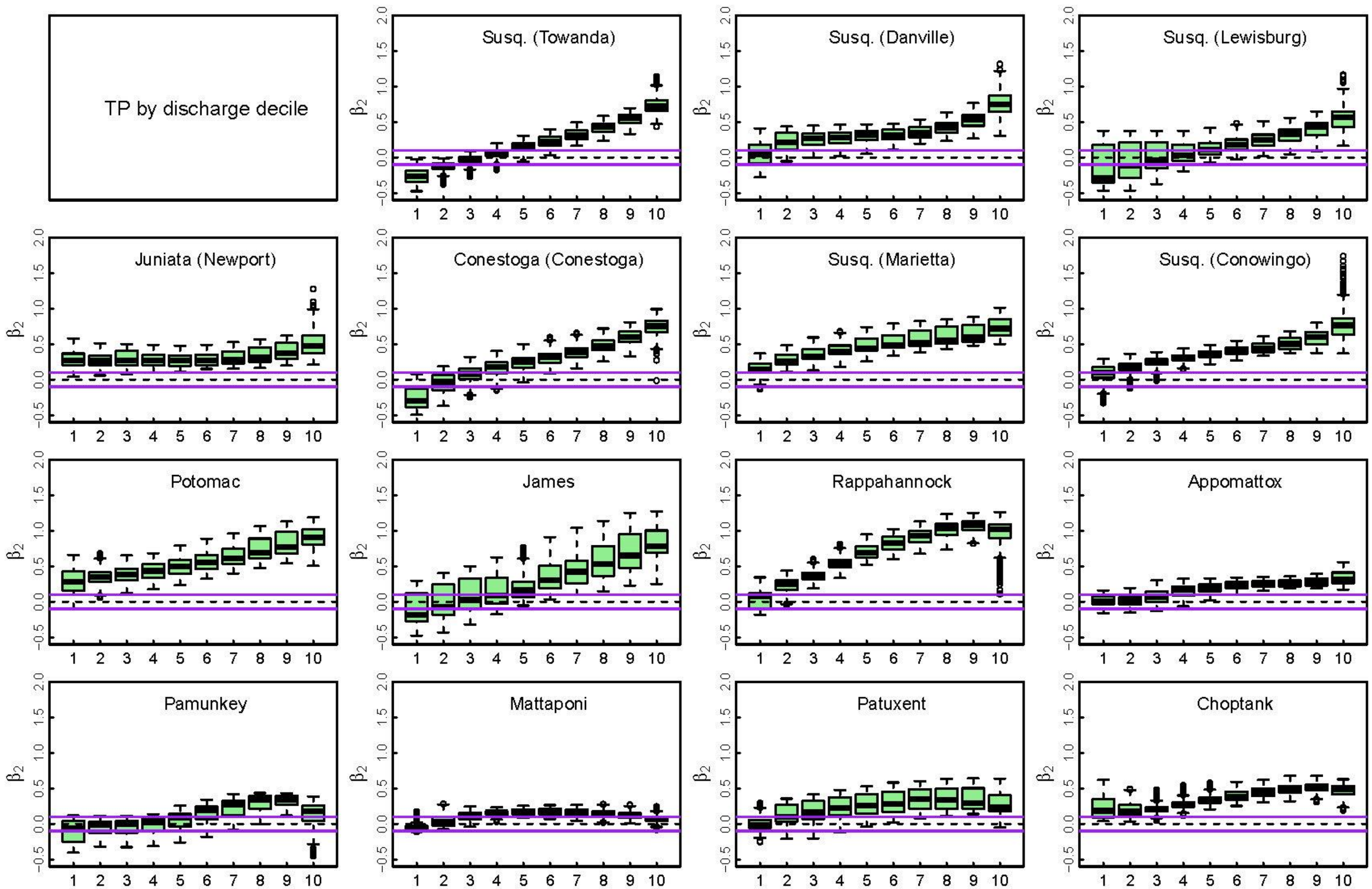

Fig. 4. Boxplot summary of estimated WRTDS β_2 coefficients by discharge decile for total phosphorus (TP) at the 15 Chesapeake sites. X-axis shows flow bins: 1 = 0^{th}~10^{th}, 2 = 10^{th}~20^{th}…, 9 = 80^{th}~90^{th}, 10 = 90^{th}~100^{th}. The region between the purple horizontal lines (*i.e.*, between -0.1 and 0.1) represents chemostasis. Regions above and below it represent mobilization and dilution, respectively.

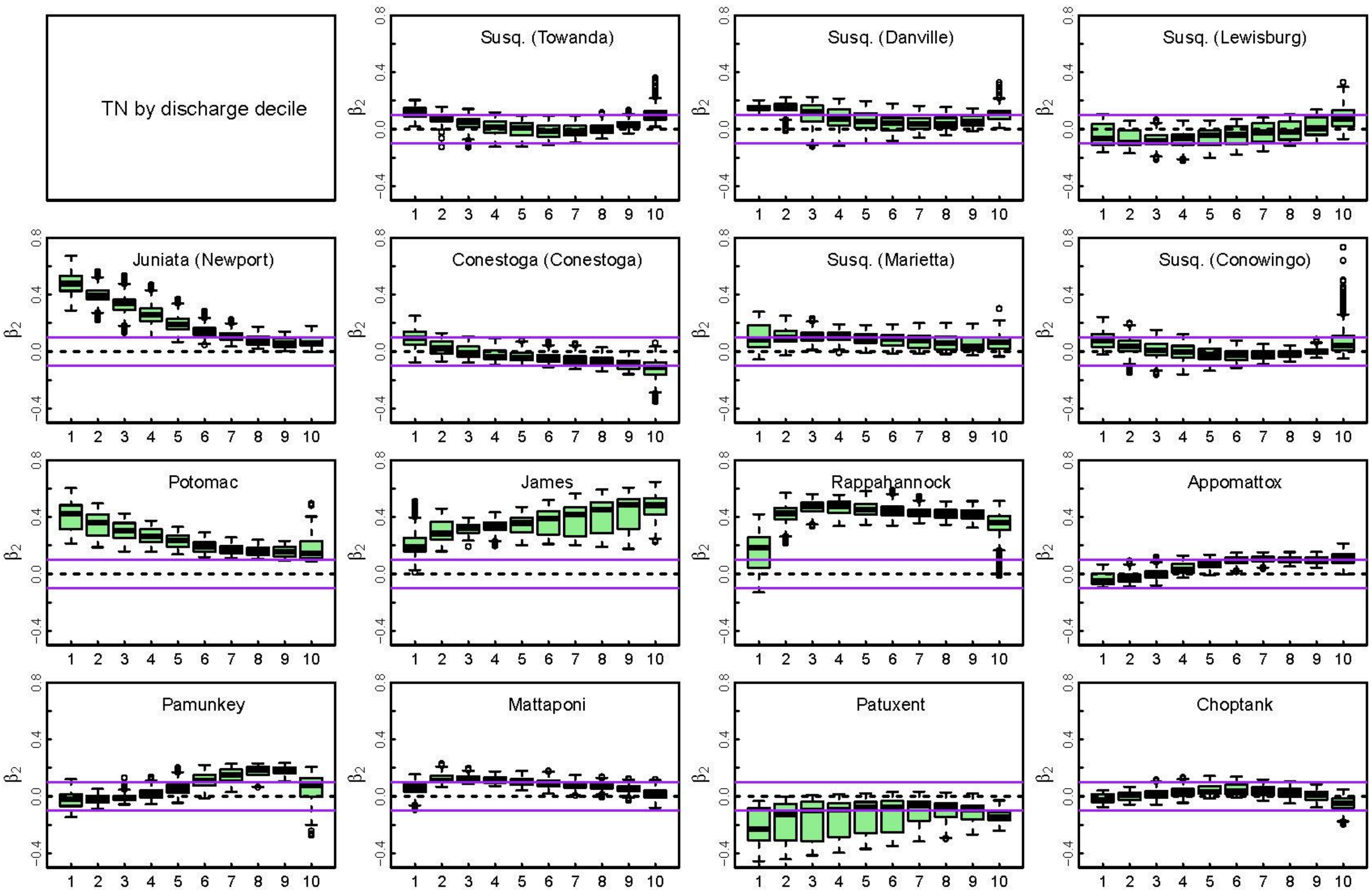

Fig. 5. Boxplot summary of estimated WRTDS β_2 coefficients by discharge decile for total nitrogen (TN) data at the 15 Chesapeake sites. X-axis shows flow bins: 1 = 0^{th}~10^{th}, 2 = 10^{th}~20^{th}…, 9 = 80^{th}~90^{th}, 10 = 90^{th}~100^{th}. The region between the purple horizontal lines (*i.e.*, between -0.1 and 0.1) represents chemostasis. Regions above and below it represent mobilization and dilution, respectively.

Table 3. Summary of comparison between low-flow ($Q_{0\text{-}10th}$; the lowest 10% of flows) and high-flow ($Q_{90\text{-}100th}$; the highest 10% of flows) *C*-*Q* patterns at the 15 Chesapeake sites. (C = chemostasis; M = mobilization; D = dilution.)

I. Summary by individual sites			
River sites	SS	TP	TN
Towanda	C-M	D-M	M-C
Danville	M-M	C-M	M-C
Lewisburg	M-M	D-M	C-C
Newport	M-M	M-M	M-C
Conestoga	M-M	D-M	C-D
Marietta	M-M	M-M	C-C
Conowingo	C-M	C-M	C-C
Potomac	M-M	M-M	M-M
James	M-M	C-M	M-M
Rappahannock	C-M	C-M	M-M
Appomattox	C-M	C-M	C-M
Pamunkey	M-M	C-M	C-C
Mattaponi	C-M	C-C	C-C
Patuxent	M-M	C-M	D-D
Choptank River	M-M	M-M	C-C
II. Summary by the nine modalities			
Modalities	SS	TP	TN
M-M	10	4	3
M-C			3
M-D			
C-M	5	7	1
C-C		1	6
C-D			1
D-M		3	
D-C			
D-D			1

3.2. Changes in *C-Q* Pattern over Time for Selected Discharge Conditions

SS coefficients have declined at 10 of the 15 sites at high discharges (**Fig. 6; Table 4**). The largest decline occurred at Pamunkey (Δ = -0.91), whereas the largest rise occurred at Conowingo (+0.81). Both changes are statistically robust based on the 50 replicate runs. Notably, the Conowingo rise is much stronger than Marietta (inlet of Conowingo Reservoir). At middle discharges, SS coefficients have declined at six sites, with the largest decline again occurred at Pamunkey (-0.35) and the largest rise at Rappahannock (+0.26). At low discharges (black lines), SS coefficients have declined at nine sites, with the largest decline occurred at Conestoga (-0.56) and the largest increase at Danville (+0.36). Among the 15 sites, four sites show declines at all three discharges (Newport, Conestoga, Pamunkey, and Choptank). Remarkably, the three largest RIM sites (Conowingo, Potomac, and James) all show rises at middle and high discharges.

TP coefficients have increased at 11 sites at high discharges (**Fig. 7; Table 4**). The largest rise again occurred at Conowingo (Δ = +0.84), whereas the largest decline occurred at Appomattox (-0.19). Both changes are robust based on the 50 replicate runs. At middle discharges, TP coefficients have increased at 11 sites, with the largest decline occurred at Choptank (-0.09) and the largest rise at James (+0.72). At low discharges, TP coefficients have increased at 11 sites, with the largest decline occurred at Choptank (-0.20) and the largest rise at Lewisburg (+0.63). Among the 15 sites, only two sites (Appomattox and Choptank) show declines at all three discharges. By contrast, eight sites show rises at all three discharges (James, Patuxent, and all Susquehanna sites except Towanda). Similar to SS, TP coefficients show rises at middle and high discharges at the three largest RIM sites.

TN coefficients have declined at nine sites at high discharges (**Fig. 8; Table 4**). The largest decline occurred at Conestoga (Δ = -0.28), whereas the largest rise occurred at Conowingo (+0.45). Both changes are robust based on the 50 replicate runs. At middle discharges, TN coefficients have declined at 10 sites, with the largest decline occurred at Choptank (-0.10) and the largest rise at Patuxent (+0.28). At low discharges, TN coefficients have declined at 9 sites, with the largest decline occurred at James (-0.18) and the largest rise at Patuxent (+0.34). Among the 15 sites, two sites (Potomac and Patuxent) show rises at all three discharges. By contrast, six sites show declines at all three discharges, including Pamunkey and all Susquehanna sites except Conowingo and Marietta. As with SS and TP, TN coefficients also show increases at high discharges at the three largest RIM sites.

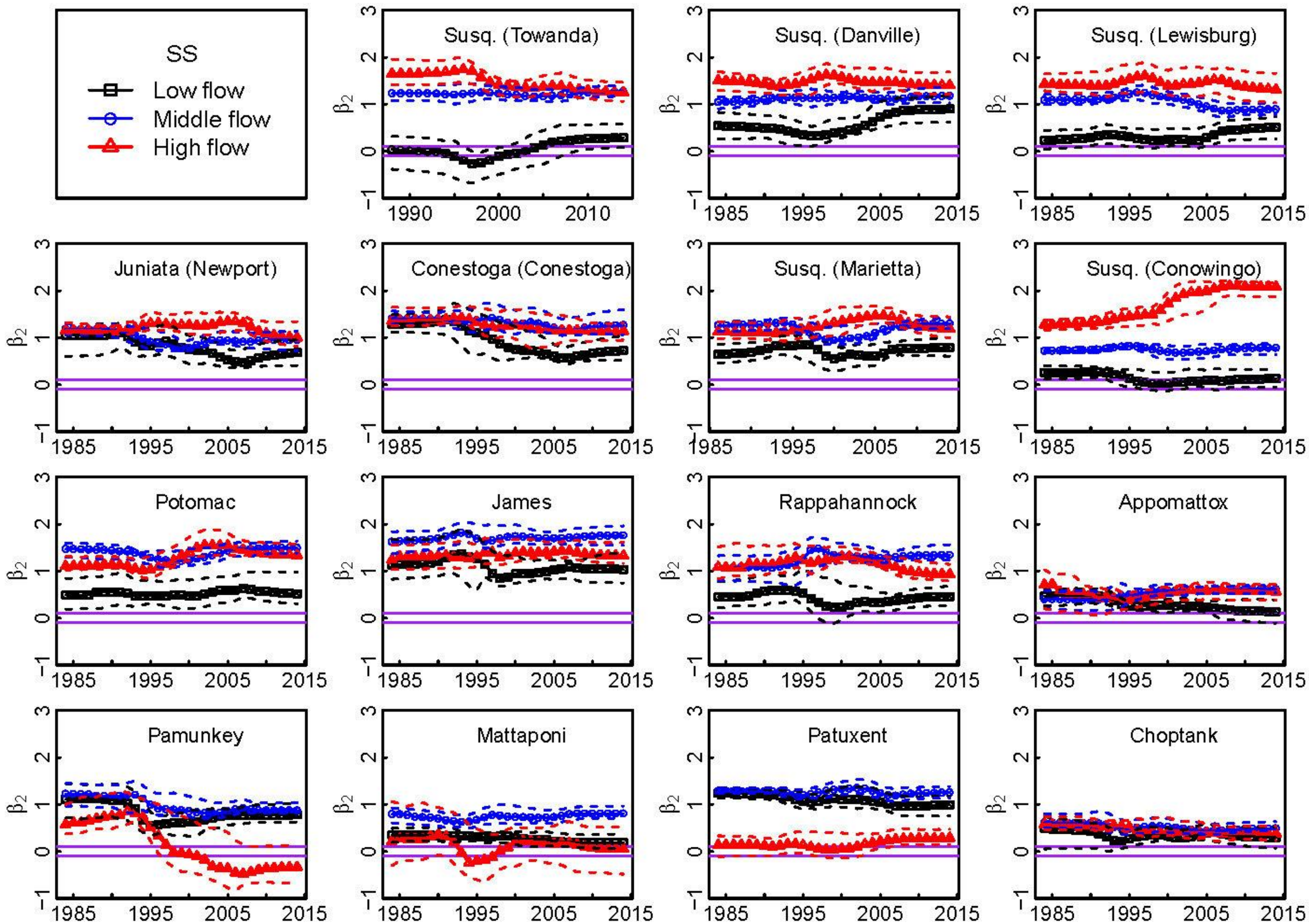

Fig. 6. Annual averages of estimated WRTDS β_2 coefficients for three selected discharges for suspended sediment (SS) at the 15 Chesapeake sites. Dashed lines represent the 90% confidence interval as derived from 50 bootstrap runs. The region between the purple horizontal lines represents chemostasis. Regions above and below it represent mobilization and dilution, respectively.

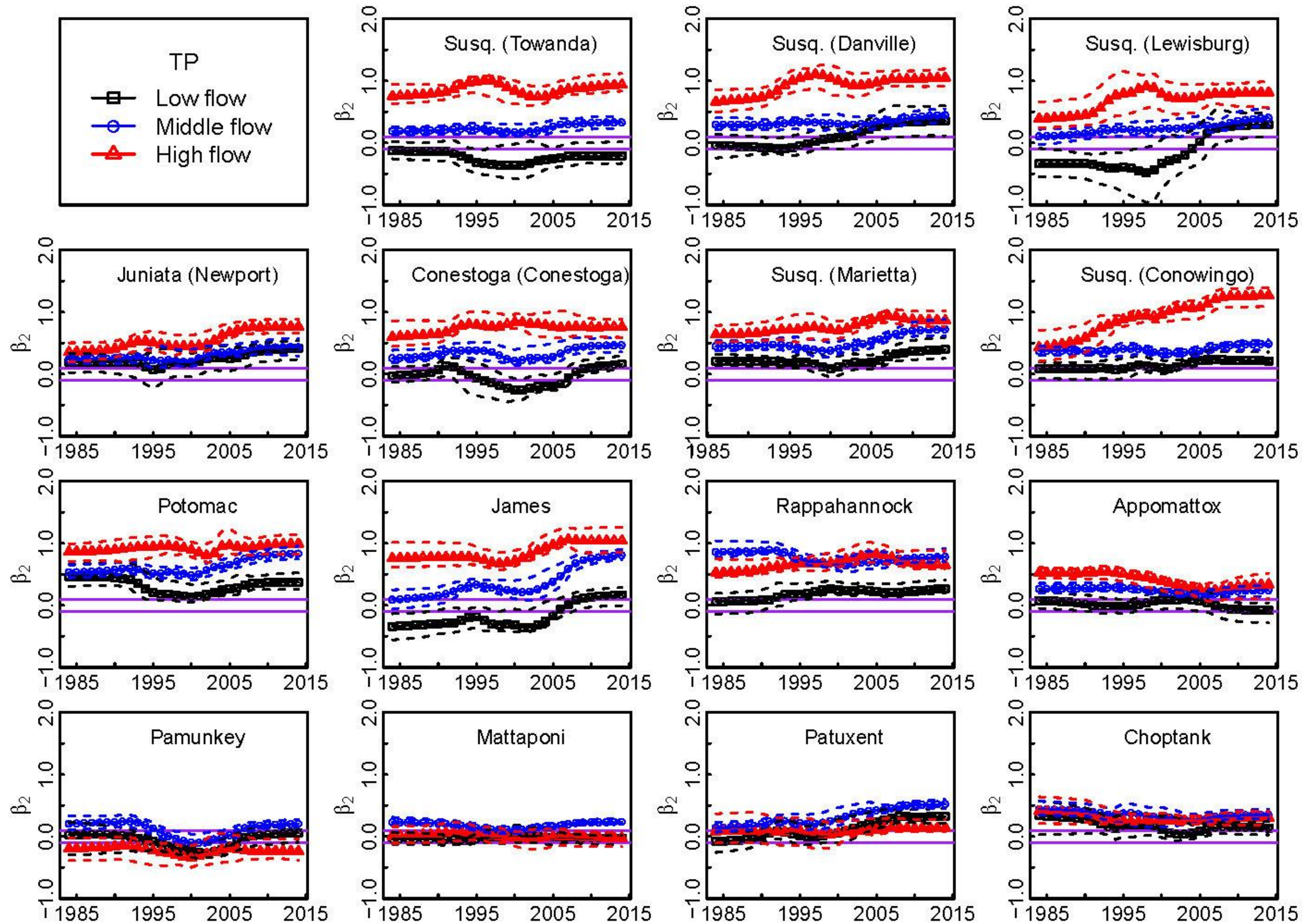

Fig. 7. Annual averages of estimated WRTDS β_2 coefficients for three selected discharges for total phosphorus (TP) at the 15 Chesapeake sites. Dashed lines represent the 90% confidence interval as derived from 50 bootstrap runs. The region between the purple horizontal lines represents chemostasis. Regions above and below it represent mobilization and dilution, respectively.

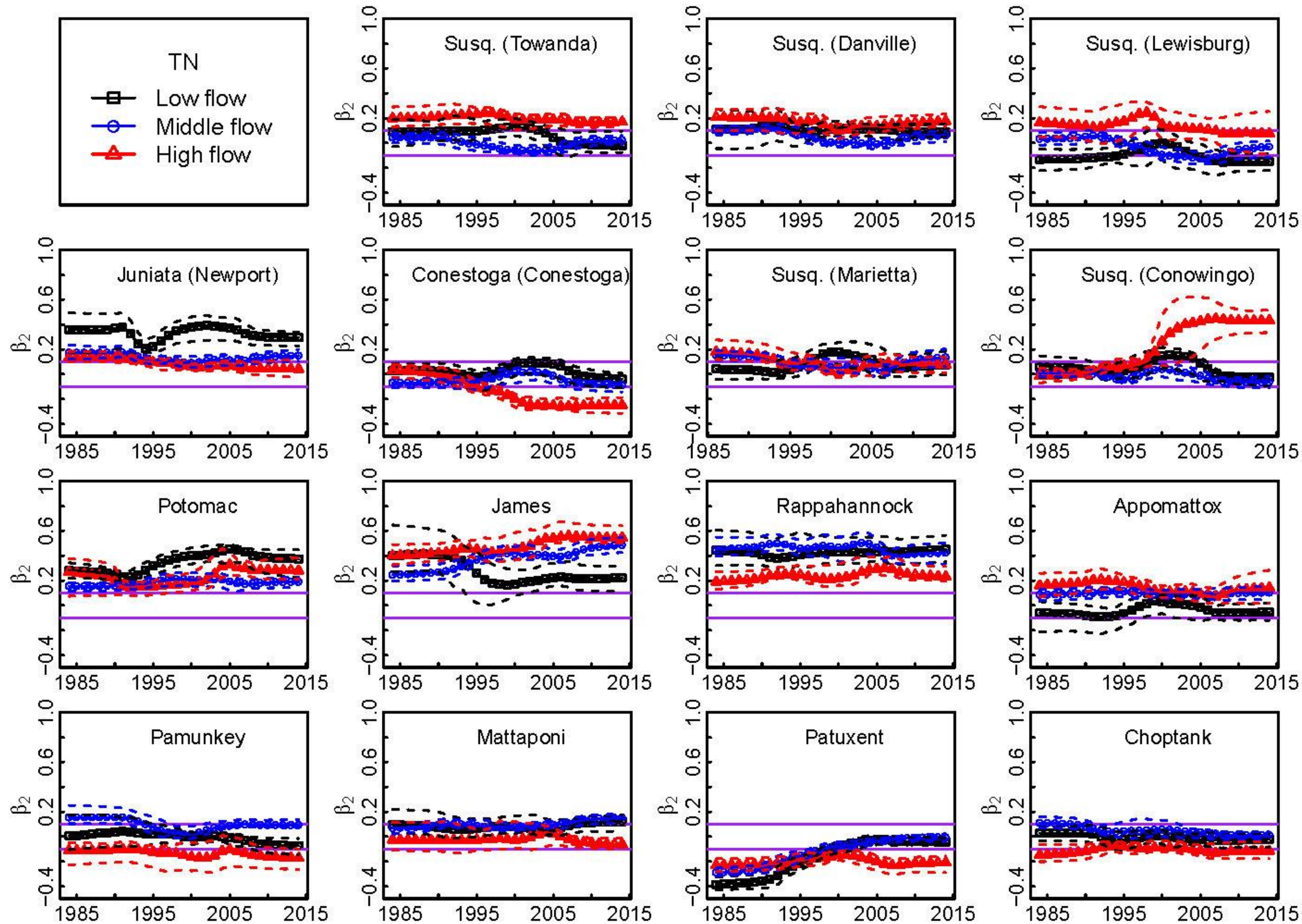

Fig. 8. Annual averages of estimated WRTDS β_2 coefficients for three selected discharges for total nitrogen (TN) at the 15 Chesapeake sites. Dashed lines represent the 90% confidence interval as derived from 50 bootstrap runs. The region between the purple horizontal lines represents chemostasis. Regions above and below it represent mobilization and dilution, respectively.

Table 4. Period-of-record changes (Δ) in estimated WRTDS β_2 coefficients at the 15 Chesapeake sites under three different discharge conditions. (Δ_{Low}: Δ under low-discharge condition; Δ_{Mid}: Δ under mid-discharge condition; Δ_{High}: Δ under high-discharge condition; $P_{\Delta>0}$: probability of positive change [Δ > 0] observed in the 50 replicate runs; pink cells: Δ > 0; green cells: Δ < 0; yellow cells: strong positive change [$P_{\Delta>0}$ > 0.9] or strong negative change [$P_{\Delta>0}$ < 0.1].)

River Sites		Suspended Sediment (SS)						Total Phosphorus (TP)						Total Nitrogen (TN)					
		Δ_{Low}	$P_{\Delta>0}$	Δ_{Mid}	$P_{\Delta>0}$	Δ_{High}	$P_{\Delta>0}$	Δ_{Low}	$P_{\Delta>0}$	Δ_{Mid}	$P_{\Delta>0}$	Δ_{High}	$P_{\Delta>0}$	Δ_{Low}	$P_{\Delta>0}$	Δ_{Mid}	$P_{\Delta>0}$	Δ_{High}	$P_{\Delta>0}$
SRBC Sites	Towanda	0.25	0.86	0.04	0.61	-0.40	0.04	-0.08	0.41	0.14	0.96	0.19	0.90	-0.11	0.16	-0.02	0.33	-0.03	0.27
	Danville	0.36	0.92	0.14	0.90	-0.10	0.31	0.40	0.98	0.15	0.92	0.39	1.00	-0.03	0.49	-0.04	0.06	-0.03	0.43
	Lewisburg	0.28	0.88	-0.20	0.00	-0.12	0.24	0.63	1.00	0.30	1.00	0.42	0.98	-0.02	0.33	-0.06	0.06	-0.09	0.25
	Newport	-0.37	0.12	-0.23	0.10	-0.15	0.29	0.22	0.88	0.20	1.00	0.41	1.00	-0.06	0.25	-0.02	0.25	-0.09	0.02
	Conestoga	-0.56	0.00	-0.14	0.25	-0.22	0.06	0.19	0.98	0.21	1.00	0.16	0.76	-0.07	0.08	-0.02	0.16	-0.28	0.00
	Marietta	0.15	0.78	0.04	0.65	0.06	0.63	0.19	0.94	0.27	1.00	0.23	0.96	0.03	0.69	-0.02	0.31	-0.11	0.02
RIM Sites	Conowingo	-0.13	0.18	0.06	0.63	0.81	1.00	0.13	0.94	0.11	0.96	0.84	1.00	-0.09	0.06	-0.07	0.02	0.45	1.00
	Potomac	0.02	0.59	0.02	0.65	0.23	0.96	-0.09	0.22	0.30	1.00	0.13	0.84	0.09	0.82	0.03	0.88	0.01	0.69
	James	-0.10	0.37	0.14	0.75	0.09	0.65	0.51	1.00	0.72	1.00	0.28	0.94	-0.18	0.06	0.24	1.00	0.15	1.00
	Rappahannock	0.01	0.53	0.26	0.90	-0.16	0.33	0.21	0.96	-0.08	0.20	0.12	0.86	0.01	0.55	-0.03	0.29	0.04	0.86
	Appomattox	-0.33	0.02	0.21	0.96	-0.15	0.59	-0.16	0.10	-0.02	0.16	-0.19	0.10	0.01	0.63	0.02	0.67	-0.02	0.33
	Pamunkey	-0.33	0.16	-0.35	0.06	-0.91	0.00	0.03	0.61	0.00	0.43	-0.04	0.45	-0.08	0.12	-0.06	0.12	-0.06	0.25
	Mattaponi	-0.16	0.18	0.01	0.71	-0.16	0.31	0.01	0.51	0.01	0.61	-0.03	0.31	0.02	0.49	0.08	0.98	-0.04	0.27
	Patuxent	-0.25	0.02	-0.03	0.31	0.15	0.86	0.40	1.00	0.38	1.00	0.06	0.75	0.34	1.00	0.28	1.00	0.02	0.59
	Choptank	-0.20	0.20	-0.12	0.20	-0.20	0.06	-0.20	0.16	-0.09	0.20	-0.11	0.14	-0.05	0.12	-0.10	0.00	0.03	0.63

4. Discussion

4.1. Changes in *C-Q* Pattern over Discharge

C-Q patterns of SS and TP show predominantly mobilization effects under a wide range of discharges (**Fig. 3-4**). This indicates that source areas across the landscape become hydrologically connected to the stream as discharge increases (Thompson *et al.*, 2012; Wolf *et al.*, 2013; Outram *et al.*, 2016). For SS and TP, nonpoint sources are likely dominant in the watersheds, otherwise dilution would have been prevalent. Mobilization observed under low-discharge and high-discharge conditions may reflect contributions by different source areas. Specifically, low-discharge mobilization more likely arises due to the flushing of sources that are near stream and/or subject to a more rapid transport pathway (*e.g.*, lateral and vertical exchanges of sediment within the hyporheic zones), whereas high-discharge mobilization more likely indicates the flushing of sources that are far from stream and/or subject to a delayed transport mechanism (*e.g.*, rill erosion). Such distinct responses may be referred to as "proximal" and "distal" responses, respectively (Sherriff *et al.*, 2016).

Deviations from the general mobilization pattern provide additional insights on SS and TP export. At low discharges, chemostasis is observed with TP at all sites and SS at five sites. This likely indicates the existence of flow thresholds for mobilization of particulate constituents, below which flow paths connecting source zones and river channel remain deactivated (Shanley *et al.*, 2011; Thompson *et al.*, 2012; Wolf *et al.*, 2013). Under such conditions, concentration is largely insensitive to flow-generation processes. At high discharges, chemostasis is rare but nonetheless observed with Mattaponi (SS and TP) and Pamunkey (TP), which implies an equilibrium between constituent supply and water flux. These cases, as well as several other cases that show decreased levels of mobilization at the high-discharge intervals (*e.g.*, SS for Patuxent; TP for Pamunkey), may reflect exhaustion of supply and/or deposition in the flood plains. In this context, the two coastal-plain rivers (Mattaponi and Choptank) behaved very differently at the high-discharge end (*i.e.*, chemostasis *vs*. mobilization). A plausible cause is the marked difference in agricultural land fraction (19% *vs*. 50%) in these two watersheds (**Table 1**).

Unlike SS and TP, TN shows predominantly chemostasis under many discharges (**Fig. 5**), which suggests that solute production and/or mobilization is nearly proportional to water flux (Godsey *et al.*, 2009; Stallard and Murphy, 2014). Dilution patterns are observed in some cases, particularly Patuxent (most discharges) and Conestoga (high discharges). Such patterns highlight the dominance of point-source contributions in these watersheds, which have the highest fractional areas of urban land among the 15 watersheds (**Table 1**). Mobilization patterns are also observed, including low-discharge conditions (Newport, Potomac, James, and Rappahannock) and high-discharge conditions (Potomac, James, Rappahannock, and Pamunkey), suggesting the dominance of nonpoint sources in these cases. Remarkably, strong mobilization is observed with Conowingo at the highest discharge but not with Marietta (inlet of Conowingo Reservoir), indicating the effect of particulate N remobilization in the reservoir (Zhang *et al.*, 2016d).

Among all three constituents, TN coefficients show the smallest variability, highlighting its distinct source and fate. In general, SS and TP are dominated by surface transport and are expected to have undergone more spatially-heterogeneous processes, *e.g.*, sources, pathways, and reactions (Heathwaite and Dils, 2000; Brakebill *et al.*, 2010; Dupas *et al.*, 2015; Zhang *et al.*, 2015). By contrast, TN is generally dominated by subsurface transport and is expected to have undergone relatively homogeneous processes due to subsurface storage and mixing over a range of spatial and temporal scales (Kirchner and Neal, 2013; Sanford and Pope, 2013; Harman, 2015). In addition, TN coefficients are generally smaller than SS and TP coefficients. The smaller sensitivities of TN concentration to discharge indicates a less important role of hydrology in N flux regulation; other factors such as biogeochemical processes may have also played important roles. A supporting evidence to this hypothesis is that median β_2 coefficients were statistically significantly (p-value < 0.05) correlated with mean summer temperature (a proxy of biogeochemical processes) at the 15 sites for TN (including all-flow, low-flow, and high-flow conditions), but not for SS or TP (data not shown). Consistent with the above findings, Moatar *et al.* (2017) also observed lower variability in *C-Q* pattern for nitrate than sediment associated constituents (including SS and TP) based on a synthesis of 200+ French sites.

Overall, export at the 15 watersheds has been dominated by mobilization for SS and TP (particulate-dominated species) and chemostasis for TN (dissolved-dominated species). The general lack of dilution patterns across most discharges may suggest that none of these species has been supply-limited. Therefore, it is legitimate to speculate that there exists sufficiently large surface and/or subsurface storage for nutrients and sediment due to legacy inputs, as previously noted on Chesapeake Bay, Mississippi River, and Lake Erie basins (Meals *et al.*, 2009; Basu *et al.*, 2010; Jarvie *et al.*, 2013; Sharpley *et al.*, 2013; Zhang *et al.*, 2016a; Van Meter *et al.*, 2017).

Finally, according to the comparison of low-flow ($Q_{0\text{-}10th}$) *vs*. high-flow ($Q_{90\text{-}100th}$) patterns (**Table 3**), all three constituents were dominated by only two or three of the nine possible modalities. Altogether, the 45 site-constituent pairs were dominated by three modalities, which are M-M (16 cases), C-M (14 cases), and C-C (7 cases), totaling 82% of all cases. In this regard, Moatar *et al.* (2017) also compared low-flow and high-flow patterns (using $Q_{0\text{-}50th}$ and $Q_{50\text{-}100th}$ intervals) and reported that these constituents were dominated by only two or three of the nine possible modalities. The authors hypothesized that intrinsic and extrinsic properties of constituent (*e.g.*, solubility, reactivity, source) fundamentally determine the basic *C-Q* pattern, which is secondarily influenced by biogeochemical activities (*e.g.*, oxic state), hydrological conditions (*e.g.*, flow path), and watershed characteristics (*e.g.*, land use). The results from this work, representative of markedly different regions, provide additional support to that conclusion. While this work was intended to seek common patterns among the watersheds, further research is needed to explore factors that have driven the unique behavior of each individual watershed, which may include watershed input, land use, reservoir density, and flood-plain structure.

4.2. Changes in *C-Q* Pattern over Time for Selected Discharge Conditions

Long-term changes in *C-Q* relationship were diverse under low-, mid-, and high- discharge conditions, which may reflect temporal shifts in watershed function due to anthropogenic activities. For the selected discharges, SS coefficients show mixed trends across sites (**Fig. 6; Table 4**). One of the most remarkable trends is Pamunkey at high discharge. This dramatic decline has caused the SS pattern to switch from mobilization to dilution, suggesting decreased availability of nonpoint sources in this watershed. Another notable pattern is the consistent decline under all three discharges at four sites (Newport, Conestoga, Pamunkey, and Choptank), presumably reflecting combined reductions of a wide range of nonpoint sources (proximal and distal). By contrast, the three largest RIM sites (*i.e.*, Susquehanna [Conowingo], Potomac, and James) show increases in β_2 at middle and high discharges, all with high confidence ($P_{\Delta>0}$ = 0.65~1.0). The rise at Conowingo is remarkable and statistically robust ($P_{\Delta>0}$ = 1.0). Considering that the Marietta coefficient has remained almost unchanged, the Conowingo rise signifies the diminished trapping efficiency of Conowingo Reservoir, as documented previously using other approaches (Hirsch, 2012; Zhang *et al.*, 2013; Zhang *et al.*, 2016d). The rises at Potomac and James may reflect combined effects of land clearance and urbanization (Brakebill *et al.*, 2010), removal of small mill dams (Walter and Merritts, 2008; Merritts *et al.*, 2011), and altered rainfall and watershed conditions that may promote erosion and transport (Karl and Knight, 1998), which deserve further investigation.

For TP coefficients, upward trends are most common (**Fig. 7; Table 4**). The Conowingo rise at high discharge is most remarkable and statistically robust ($P_{\Delta>0}$ = 1.0). This rise is also much larger than that of Marietta and thus corroborates the reservoir effect discussed above. Moreover, TP coefficients have increased at high discharges at the four largest RIM sites (Conowingo, Potomac, James, and Rappahannock), all with high confidence ($P_{\Delta>0}$ = 0.84~1.0). This is alarming since the four sites represent a vast majority of the nontidal Bay watershed. Several sites show major shifts in TP pattern at low discharges: Lewisburg and James switched from dilution to mobilization, whereas Danville, Conowingo, Rappahannock, and Patuxent switched from chemostasis to mobilization. These shifts probably suggest enrichment of nonpoint sources over the record and/or depletion of point sources due to management actions such as P-detergent ban (Litke, 1999) and enhanced nutrient removal at wastewater treatment plants (Sprague *et al.*, 2000; Boynton *et al.*, 2008). Reverse effects occurred at Choptank, where the low-discharge pattern switched from mobilization to chemostasis, reflecting decreased dominance of nonpoint sources or exhaustion of such sources.

For TN coefficients, downward trends are most common (**Fig. 8; Table 4**). Among all sites, the largest decline is observed with Conestoga at high discharge and with high confidence ($P_{\Delta<0}$ = 1.0). Interestingly, its pattern has shifted from mobilization to dilution. Such change may reflect the effectiveness of nonpoint source reductions in this mixed-land-use watershed. By contrast, TN coefficients have increased at high discharges in the four largest RIM sites, all with high confidence ($P_{\Delta>0}$ = 0.69~1.0). The most significant rise is observed with Conowingo at high discharge, which has caused the pattern to switch from chemostasis to mobilization. The implication is that N concentration in the reservoir effluent has become more sensitive to discharge as the reservoir approaches sediment storage capacity (Langland, 2015). Six sites show declines in coefficients at all three discharges (Pamunkey and five Susquehanna sites), reflecting reduced sensitivity to discharge that was probably attributable to reduction of nonpoint sources and atmospheric sources in these watersheds (Linker *et al.*, 2013). By contrast, Potomac and Patuxent both show rises at all three discharges, which have followed different mechanisms. For Potomac, the coefficients have become more positive, suggesting increased nonpoint source dominance. For Patuxent, the coefficients have become less negative, suggesting decreased point-source dominance due to technology upgrade at wastewater treatment plants (Sprague *et al.*, 2000; Boynton *et al.*, 2008).

Overall, these changes in coefficients demonstrate clear temporal non-stationarity in *C*-*Q* patterns at the 15 Chesapeake sites. Such non-stationary relationships effectively highlight the complexity of watershed function, which should be taken into consideration when riverine *C*-*Q* data sets are used to infer transport processes or estimate concentrations and fluxes using regression approaches (Horowitz, 2003; Crowder *et al.*, 2007; Hirsch *et al.*, 2010; Hirsch, 2014). The diverse trends in *C*-*Q* patterns under different discharge conditions may reflect major changes in dominant watershed sources due to anthropogenic actions. Future research should investigate factors that have driven the observed changes in the various watersheds. In addition, from a multiple-method perspective toward watershed management, these trends in WRTDS coefficients may be compared with other approaches (*e.g.*, WRTDS flow-normalization, seasonal Kendall test) to identify consistent conclusions on water-quality conditions and changes.

5. Conclusions

Through a synthesis of *C*-*Q* patterns for nine major tributaries of Chesapeake Bay, this work has provided several new insights on the complexity of watershed function (*i.e.*, the sensitivity of concentration to discharge). Results show that constituent export at the 15 long-term sites has been dominated by mobilization patterns for SS and TP (particulate-dominated species) and chemostasis patterns for TN (dissolved-dominated species) under many discharge conditions. Among the nine possible modalities of low-flow *vs*. high-flow patterns, the three most frequent modalities are mobilization-mobilization (17 cases), chemostasis-mobilization (13 cases), and chemostasis-chemostasis (7 cases), representing 82% of all 45 watershed-constituent pairs. The general lack of dilution patterns may suggest that none of these constituents has been supply-limited in these watersheds. Moreover, for many site-constituent combinations, coefficients show clear temporal non-stationarity in *C*-*Q* relationships under various discharge conditions, reflecting major changes in dominant watershed sources due to anthropogenic actions. These results also highlight the potential pitfalls of assuming fixed *C*-*Q* relationships in the record. Continued research is needed to investigate factors that have driven the observed water-quality changes in the various watersheds under different discharges.

This work demonstrates the utility of the WRTDS model coefficients to provide informative interpretation of *C*-*Q* relationships in discretely-sampled data. Unlike many previous *C*-*Q* studies that focused on stormflow conditions, this approach allows simultaneous examination of various discharge conditions. In addition, this work illustrates the value of adopting a top-down approach for synthesizing temporal and spatial patterns of *C*-*Q* relationships across multiple watersheds, in order to infer the status and changes of constituent export as well as the relative dominance of sources under different flow conditions. In this regard, WRTDS coefficients provide a useful means for generation of sensible hypothesis on dominant processes in different watersheds. Moreover, the synthesis on *C*-*Q* temporal patterns was conducted within an uncertainty framework to provide sound conclusions, which is presumably the first of its kind. Broadly, the approach demonstrated here is readily adaptable to other river systems, where long-term discretely-sampled data are available, to decipher complex interactions between hydrological and biogeochemical processes.

Acknowledgements

This work was supported by the Maryland Sea Grant (NA10OAR4170072; NA14OAR1470090), Maryland Water Resources Research Center (2015MD329B), and National Science Foundation (CBET-1360415) when Zhang was a doctoral student at Johns Hopkins University. Additional support was provided by the U.S. Environmental Protection Agency under grant "EPA/CBP Technical Support 2017" (No. 07-5-230480). Zhang is deeply indebted to his Ph.D advisor, Dr. William Ball, for his advice and guidance. The author also acknowledges Dano Wilusz (JHU) for insightful discussions and Andrew Sekellick (USGS) for assistance on the map (Fig. 1).

References

Basu, N. B., G. Destouni, J. W. Jawitz, S. E. Thompson, N. V. Loukinova, A. Darracq, S. Zanardo, M. Yaeger, M. Sivapalan, A. Rinaldo and P. S. C. Rao, 2010. Nutrient loads exported from managed catchments reveal emergent biogeochemical stationarity. *Geophys. Res. Lett.* 37:L23404, DOI: 10.1029/2010gl045168.

Basu, N. B., S. E. Thompson and P. S. C. Rao, 2011. Hydrologic and biogeochemical functioning of intensively managed catchments: A synthesis of top-down analyses. *Water Resour. Res.* 47:W00J15, DOI: 10.1029/2011WR010800.

Bieroza, M. Z. and A. L. Heathwaite, 2015. Seasonal variation in phosphorus concentration–discharge hysteresis inferred from high-frequency in situ monitoring. *Journal of Hydrology* 524:333-347, DOI: 10.1016/j.jhydrol.2015.02.036.

Bowes, M. J., J. T. Smith, H. P. Jarvie and C. Neal, 2008. Modelling of phosphorus inputs to rivers from diffuse and point sources. *Sci. Total Environ.* 395:125-138, DOI: 10.1016/j.scitotenv.2008.01.054.

Bowes, M. J., J. T. Smith, H. P. Jarvie, C. Neal and R. Barden, 2009. Changes in point and diffuse source phosphorus inputs to the River Frome (Dorset, UK) from 1966 to 2006. *Sci. Total Environ.* 407:1954-1966, DOI: 10.1016/j.scitotenv.2008.11.026.

Boynton, W. R., J. D. Hagy, J. C. Cornwell, W. M. Kemp, S. M. Greene, M. S. Owens, J. E. Baker and R. K. Larsen, 2008. Nutrient Budgets and Management Actions in the Patuxent River Estuary, Maryland. *Estuaries Coasts* 31:623-651, DOI: 10.1007/s12237-008-9052-9.

Brakebill, J. W., S. W. Ator and G. E. Schwarz, 2010. Sources of suspended-sediment flux in streams of the Chesapeake Bay Watershed: A regional application of the SPARROW model. *J. Am. Water Resour. Assoc.* 46:757-776, DOI: 10.1111/j.1752-1688.2010.00450.x.

Burt, T. P., F. Worrall, N. J. K. Howden and M. G. Anderson, 2015. Shifts in discharge-concentration relationships as a small catchment recover from severe drought. *Hydrol. Process.* 29:498-507, DOI: 10.1002/hyp.10169.

Chanat, J. G., D. L. Moyer, J. D. Blomquist, K. E. Hyer and M. J. Langland, 2016. Application of a weighted regression model for reporting nutrient and sediment concentrations, fluxes, and trends in concentration and flux for the Chesapeake Bay Nontidal Water-Quality Monitoring Network, results through water year 2012. U.S. Geological Survey Scientific Investigations Report 2015-5133, Reston, VA, p. 76. http://dx.doi.org/10.3133/sir20155133.

Chanat, J. G., K. C. Rice and G. M. Hornberger, 2002. Consistency of patterns in concentration-discharge plots. *Water Resour. Res.* 38:1-10, DOI: 10.1029/2001WR000971.

Crowder, D. W., M. Demissie and M. Markus, 2007. The accuracy of sediment loads when log-transformation produces nonlinear sediment load–discharge relationships. *Journal of Hydrology* 336:250-268, DOI: 10.1016/j.jhydrol.2006.12.024.

Dupas, R., C. Gascuel-Odoux, N. Gilliet, C. Grimaldi and G. Gruau, 2015. Distinct export dynamics for dissolved and particulate phosphorus reveal independent transport mechanisms in an arable headwater catchment. *Hydrol. Process.* 29:3162–3178, DOI: 10.1002/hyp.10432.

Evans, C. and T. D. Davies, 1998. Causes of concentration/discharge hysteresis and its potential as a tool for analysis of episode hydrochemistry. *Water Resour. Res.* 34:129-137, DOI:

10.1029/97WR01881.

Godsey, S. E., J. W. Kirchner and D. W. Clow, 2009. Concentration-discharge relationships reflect chemostatic characteristics of US catchments. *Hydrol. Process.* 23:1844-1864, DOI: 10.1002/hyp.7315.

Gray, A. B., G. B. Pasternack, E. B. Watson, J. A. Warrick and M. A. Goñi, 2015. Effects of antecedent hydrologic conditions, time dependence, and climate cycles on the suspended sediment load of the Salinas River, California. *Journal of Hydrology* 525:632-649, DOI: 10.1016/j.jhydrol.2015.04.025.

Harman, C. J., 2015. Time-variable transit time distributions and transport: Theory and application to storage-dependent transport of chloride in a watershed. *Water Resour. Res.* 51:1–30, DOI: 10.1002/2014WR015707.

Heathwaite, A. and R. Dils, 2000. Characterising phosphorus loss in surface and subsurface hydrological pathways. *Sci. Total Environ.* 251-252:523-538, DOI: 10.1016/S0048-9697(00)00393-4.

Herndon, E. M., A. L. Dere, P. L. Sullivan, D. Norris, B. Reynolds and S. L. Brantley, 2015. Landscape heterogeneity drives contrasting concentration–discharge relationships in shale headwater catchments. *Hydrol. Earth Syst. Sci.* 19:3333-3347, DOI: 10.5194/hess-19-3333-2015.

Hirsch, R. M., 2012. Flux of Nitrogen, Phosphorus, and Suspended Sediment from the Susquehanna River Basin to the Chesapeake Bay during Tropical Storm Lee, September 2011, as an indicator of the effects of reservoir sedimentation on water quality. U.S. Geological Survey Scientific Investigations Report 2012-5185, Reston, VA, p. 17. http://pubs.usgs.gov/sir/2012/5185/.

Hirsch, R. M., 2014. Large Biases in Regression-Based Constituent Flux Estimates: Causes and Diagnostic Tools. *J. Am. Water Resour. Assoc.* 50:1401-1424, DOI: 10.1111/jawr.12195.

Hirsch, R. M., S. A. Archfield and L. A. De Cicco, 2015. A bootstrap method for estimating uncertainty of water quality trends. *Journal of Environmental Modelling and Software* 73:148-166, DOI: 10.1016/j.envsoft.2015.07.017.

Hirsch, R. M. and L. De Cicco, 2015. User guide to Exploration and Graphics for RivEr Trends (EGRET) and dataRetrieval: R packages for hydrologic data (version 2.0, February 2015). U.S. Geological Survey Techniques and Methods Book 4, Chapter A10, Reston, VA, p. 93. http://dx.doi.org/10.3133/tm4A10.

Hirsch, R. M., D. L. Moyer and S. A. Archfield, 2010. Weighted regressions on time, discharge, and season (WRTDS), with an application to Chesapeake Bay river inputs. *J. Am. Water Resour. Assoc.* 46:857-880, DOI: 10.1111/j.1752-1688.2010.00482.x.

Horowitz, A. J., 2003. An evaluation of sediment rating curves for estimating suspended sediment concentrations for subsequent flux calculations. *Hydrol. Process.* 17:3387-3409, DOI:

10.1002/hyp.1299.

House, W. A. and M. S. Warwick, 1998. Hysteresis of the solute concentration/discharge relationship in rivers during storms. *Water Res.* 32:2279-2290, DOI: 10.1016/S0043-1354(97)00473-9.

Jarvie, H. P., A. N. Sharpley, B. Spears, A. R. Buda, L. May and P. J. A. Kleinman, 2013. Water Quality Remediation Faces Unprecedented Challenges from “Legacy Phosphorus”. *Environ. Sci. Technol.* 47:8997-8998, DOI: 10.1021/es403160a.

Karl, T. R. and R. W. Knight, 1998. Secular Trends of Precipitation Amount, Frequency, and Intensity in the United States. *Bull. Am. Meteorol. Soc.* 79:231-241, DOI: 10.1175/1520-0477(1998)079<0231:STOPAF>2.0.CO;2.

Kemp, W. M., W. R. Boynton, J. E. Adolf, D. F. Boesch, W. C. Boicourt, G. Brush, J. C. Cornwell, T. R. Fisher, P. M. Glibert, J. D. Hagy, L. W. Harding, E. D. Houde, D. G. Kimmel, W. D. Miller, R. I. E. Newell, M. R. Roman, E. M. Smith and J. C. Stevenson, 2005. Eutrophication of Chesapeake Bay: historical trends and ecological interactions. *Mar. Ecol. Prog. Ser.* 303:1-29, DOI: 10.3354/meps303001.

Kirchner, J. W. and C. Neal, 2013. Universal fractal scaling in stream chemistry and its implications for solute transport and water quality trend detection. *Proc. Natl. Acad. Sci. U. S. A.* 110:12213-12218, DOI: 10.1073/pnas.1304328110.

Kutner, M., C. Nachtsheim and J. Neter, 2004. *Applied Linear Statistical Models*, McGraw-Hill Education, ISBN 0073014664

Langland, M. J., 2015. Sediment transport and capacity change in three reservoirs, Lower Susquehanna River Basin, Pennsylvania and Maryland, 1900-2012. U.S. Geological Survey Open-File Report 2014-1235, Reston, VA, p. 18. http://dx.doi.org/10.3133/ofr20141235.

Linker, L. C., R. Dennis, G. W. Shenk, R. A. Batiuk, J. Grimm and P. Wang, 2013. Computing Atmospheric Nutrient Loads to the Chesapeake Bay Watershed and Tidal Waters. *J. Am. Water Resour. Assoc.* 49:1025-1041, DOI: 10.1111/jawr.12112.

Litke, D. W., 1999. Review of phosphorus control measures in the United States and their effects on water quality. U.S. Geological Survey Water-Resources Investigations Report 99-4007, Denver, CO, p. 43. http://pubs.usgs.gov/wri/wri994007/.

Meals, D. W., S. A. Dressing and T. E. Davenport, 2009. Lag time in water quality response to best management practices: a review. *J. Environ. Qual.* 39:85-96, DOI: 10.2134/jeq2009.0108.

Merritts, D., R. Walter, M. Rahnis, J. Hartranft, S. Cox, A. Gellis, N. Potter, W. Hilgartner, M. Langland, L. Manion, C. Lippincott, S. Siddiqui, Z. Rehman, C. Scheid, L. Kratz, A. Shilling, M. Jenschke, K. Datin, E. Cranmer, A. Reed, D. Matuszewski, M. Voli, E. Ohlson, A. Neugebauer, A. Ahamed, C. Neal, A. Winter and S. Becker, 2011. Anthropocene streams and base-level controls from historic dams in the unglaciated mid-Atlantic region, USA. *Philosophical Transactions of the Royal Society A* 369:976-1009, DOI: 10.1098/rsta.2010.0335.

Meybeck, M. and F. Moatar, 2012. Daily variability of river concentrations and fluxes: Indicators based on the segmentation of the rating curve. *Hydrol. Process.* 26:1188-1207, DOI: 10.1002/hyp.8211.

Moatar, F., B. Abbott, C. Minaudo, F. Curie and G. Pinay, 2017. Elemental properties, hydrology, and biology interact to shape concentration-discharge curves for carbon, nutrients, sediment, and major ions. *Water Resour. Res.* 53, DOI: 10.1002/2016WR019635.

Murphy, R. R., W. M. Kemp and W. P. Ball, 2011. Long-term trends in Chesapeake Bay seasonal hypoxia, stratification, and nutrient loading. *Estuaries Coasts* 34:1293-1309, DOI: 10.1007/s12237-011-9413-7.

Musolff, A., C. Schmidt, B. Selle and J. H. Fleckenstein, 2015. Catchment controls on solute export. *Adv. Water Resour.* 86:133-146, DOI: 10.1016/j.advwatres.2015.09.026.

Outram, F. N., R. J. Cooper, G. Sünnenberg, K. M. Hiscock and A. A. Lovett, 2016. Antecedent conditions , hydrological connectivity and anthropogenic inputs : Factors affecting nitrate and phosphorus transfers to agricultural headwater streams. *Sci. Total Environ.* 546:184-199, DOI: 10.1016/j.scitotenv.2015.12.025.

Outram, F. N., C. E. M. Lloyd, J. Jonczyk, C. M. H. Benskin, F. Grant, M. T. Perks, C. Deasy, S. P. Burke, A. L. Collins, J. Freer, P. M. Haygarth, K. M. Hiscock, P. J. Johnes and A. L. Lovett, 2014. High-frequency monitoring of nitrogen and phosphorus response in three rural catchments to the end of the 2011–2012 drought in England. *Hydrol. Earth Syst. Sci.* 18:3429-3448, DOI: 10.5194/hess-18-3429-2014.

R Development Core Team, 2014. R: A language and environment for statistical computing. R Foundation for Statistical Computing, Vienna, Austria. ISBN 3900051070. http://www.r-project.org.

Sanford, W. E. and J. P. Pope, 2013. Quantifying Groundwater's Role in Delaying Improvements to Chesapeake Bay Water Quality. *Environ. Sci. Technol.* 47:13330-13338, DOI: 10.1021/es401334k.

Shanley, J. B., W. H. McDowell and R. F. Stallard, 2011. Long-term patterns and short-term dynamics of stream solutes and suspended sediment in a rapidly weathering tropical watershed. *Water Resour. Res.* 47:W07515, DOI: 10.1029/2010WR009788.

Sharpley, A., H. P. Jarvie, A. Buda, L. May, B. Spears and P. Kleinman, 2013. Phosphorus Legacy: Overcoming the Effects of Past Management Practices to Mitigate Future Water Quality Impairment. *J. Environ. Qual.* 42:1308–1326, DOI: 10.2134/jeq2013.03.0098.

Shenk, G. W. and L. C. Linker, 2013. Development and Application of the 2010 Chesapeake Bay Watershed Total Maximum Daily Load Model. *J. Am. Water Resour. Assoc.* 49:1042-1056, DOI: 10.1111/jawr.12109.

Sherriff, S. C., J. S. Rowan, O. Fenton, P. Jordan, A. R. Melland, P.-E. Mellander and D. Ó. hUallacháin, 2016. Storm Event Suspended Sediment-Discharge Hysteresis and Controls in Agricultural Watersheds: Implications for Watershed Scale Sediment Management. *Environ. Sci. Technol.* 50:1769-1778, DOI: 10.1021/acs.est.5b04573.

Sprague, L. A., M. J. Langland, S. E. Yochum, R. E. Edwards, J. D. Blomquist, S. W. Phillips, G. W. Shenk and S. D. Preston, 2000. Factors affecting nutrient trends in major rivers of the Chesapeake Bay Watershed. U.S. Geological Survey Water-Resources Investigations Report 00-4218, Richmond, VA, p. 109. http://va.water.usgs.gov/online_pubs/WRIR/00-4218.htm.

Stallard, R. F. and S. F. Murphy, 2014. A Unified Assessment of Hydrologic and Biogeochemical Responses in Research Watersheds in Eastern Puerto Rico Using Runoff-Concentration Relations. *Aquat. Geochem.* 20:115-139, DOI: 10.1007/s10498-013-9216-5.

Susquehanna River Basin Commission, 2014. Sediment and nutrient assessment program. http://www.srbc.net/programs/cbp/nutrientprogram.htm.

Thompson, J. J. D., D. G. Doody, R. Flynn and C. J. Watson, 2012. Dynamics of critical source areas: does connectivity explain chemistry? *Sci. Total Environ.* 435-436:499-508, DOI: 10.1016/j.scitotenv.2012.06.104.

Thompson, S. E., N. B. Basu, J. Lascurain, A. Aubeneau and P. S. C. Rao, 2011. Relative dominance of hydrologic versus biogeochemical factors on solute export across impact gradients. *Water Resour. Res.* 47:W00J05, DOI: 10.1029/2010WR009605.

U.S. Geological Survey, 2014. Surface-water data for the nation.

Van Meter, K. J., N. B. Basu and P. Van Cappellen, 2017. Two Centuries of Nitrogen Dynamics: Legacy Sources and Sinks in the Mississippi and Susquehanna River Basins. *Global Biogeochem. Cycles* 31:2-23, DOI: 10.1002/2016GB005498.

Walter, R. C. and D. J. Merritts, 2008. Natural streams and the legacy of water-powered mills. *Science* 319:299-304, DOI: 10.1126/science.1151716.

Wolf, K. L., G. B. Noe and C. Ahn, 2013. Hydrologic Connectivity to Streams Increases Nitrogen and Phosphorus Inputs and Cycling in Soils of Created and Natural Floodplain Wetlands. *J. Environ. Qual.* 42:1245-1255, DOI: 10.2134/jeq2012.0466.

Zhang, Q., W. P. Ball and D. L. Moyer, 2016a. Decadal-scale export of nitrogen, phosphorus, and sediment from the Susquehanna River basin, USA: Analysis and synthesis of temporal and spatial patterns. *Sci. Total Environ.* 563-564:1016-1029, DOI: 10.1016/j.scitotenv.2016.03.104.

Zhang, Q., D. C. Brady and W. P. Ball, 2013. Long-term seasonal trends of nitrogen, phosphorus, and suspended sediment load from the non-tidal Susquehanna River Basin to Chesapeake Bay. *Sci. Total Environ.* 452-453:208-221, DOI: 10.1016/j.scitotenv.2013.02.012.

Zhang, Q., D. C. Brady, W. Boynton and W. P. Ball, 2015. Long-term Trends of Nutrients and Sediment from the Nontidal Chesapeake Watershed: An Assessment of Progress by River and Season. *J. Am. Water Resour. Assoc.* 51:1534-1555, DOI: 10.1111/1752-1688.12327.

Zhang, Q., C. J. Harman and W. P. Ball, 2016b. Data associated with An Improved Method for Interpretation of Riverine Concentration-Discharge Relationships Indicates Long-Term Shifts in Reservoir Sediment Trapping. Baltimore, MD, Johns Hopkins University Data Archive. http://dx.doi.org/10.7281/T18G8HM0, DOI: 10.7281/T18G8HM0.

Zhang, Q., C. J. Harman and W. P. Ball, 2016c. An Improved Method for Interpretation of Riverine Concentration-Discharge Relationships Indicates Long-Term Shifts in Reservoir Sediment Trapping. *Geophys. Res. Lett.* 43:10215-10224, DOI: 10.1002/2016GL069945.

Zhang, Q., R. M. Hirsch and W. P. Ball, 2016d. Long-Term Changes in Sediment and Nutrient Delivery from Conowingo Dam to Chesapeake Bay: Effects of Reservoir Sedimentation. *Environ. Sci. Technol.* 50:1877-1886, DOI: 10.1021/acs.est.5b04073.

List of Tables and Figures

Table 1. Details of the 15 long-term monitoring sites in the Chesapeake Bay watershed.

Table 2. Temporal coverage of observed water-quality data at the 15 Chesapeake sites.

Table 3. Summary of contrast between low-flow (i.e., $Q_{0\text{-}10th}$; the lowest 10% of flows) and high-flow (i.e., $Q_{90\text{-}100th}$; the highest 10% of flows) C-Q patterns at the 15 Chesapeake sites.

Table 4. Period-of-record changes (Δ) in estimated WRTDS β_2 coefficients at the 15 Chesapeake sites under three different discharge conditions.

Fig. 1. Chesapeake Bay watershed and the 15 monitoring sites that include nine River Input Monitoring (RIM) sites on the fall-line of nine major tributaries and six Susquehanna River Basin Commission (SRBC) sites at upstream locations within the Susquehanna River basin.

Fig. 2. Contour plot showing estimated WRTDS β_2 coefficients as a function of time and discharge for total phosphorus in Susquehanna River at Conowingo, MD. Black open circles indicate the time-discharge combinations where concentration samples have been taken. The β_2 coefficients correspond to three broad categories, namely, (1) dilution *(i.e.*, $\beta_2 < 0$); (2) chemostasis ($\beta_2 \approx 0$); and (3) mobilization ($\beta_2 > 0$).

Fig. 3. Boxplot summary of estimated WRTDS β_2 coefficients by discharge decile for suspended sediment (SS) at the 15 Chesapeake sites. X-axis shows flow bins: 1 = 0^{th}~10^{th}, 2 =

10^{th}~20^{th}…, 9 = 80^{th}~90^{th}, and 10 = 90^{th}~100^{th}. The region between the purple horizontal lines (*i.e.*, between -0.1 and 0.1) represents chemostasis. Regions above and below it represent mobilization and dilution, respectively.

Fig. 4. Boxplot summary of estimated WRTDS β_2 coefficients by discharge decile for total phosphorus (TP) at the 15 Chesapeake sites. X-axis shows flow bins: 1 = 0^{th}~10^{th}, 2 = 10^{th}~20^{th}…, 9 = 80^{th}~90^{th}, and 10 = 90^{th}~100^{th}. The region between the purple horizontal lines (*i.e.*, between -0.1 and 0.1) represents chemostasis. Regions above and below it represent mobilization and dilution, respectively.

Fig. 5. Boxplot summary of estimated WRTDS β_2 coefficients by discharge decile for total nitrogen (TN) data at the 15 Chesapeake sites. X-axis shows flow bins: 1 = 0^{th}~10^{th}, 2 = 10^{th}~20^{th}…, 9 = 80^{th}~90^{th}, and 10 = 90^{th}~100^{th}. The region between the purple horizontal lines (*i.e.*, between -0.1 and 0.1) represents chemostasis. Regions above and below it represent mobilization and dilution, respectively.

Fig. 6. Annual averages of estimated WRTDS β_2 coefficients for three selected discharges for suspended sediment (SS) at the 15 Chesapeake sites. Dashed lines represent the 90% confidence interval as derived from 50 bootstrap runs. The region between the purple horizontal lines represents chemostasis. Regions above and below it represent mobilization and dilution, respectively.

Fig. 7. Annual averages of estimated WRTDS β_2 coefficients for three selected discharges for total phosphorus (TP) at the 15 Chesapeake sites. Dashed lines represent the 90% confidence interval as derived from 50 bootstrap runs. The region between the purple horizontal lines represents chemostasis. Regions above and below it represent mobilization and dilution, respectively.

Fig. 8. Annual averages of estimated WRTDS β_2 coefficients for three selected discharges for total nitrogen (TN) at the 15 Chesapeake sites. Dashed lines represent the 90% confidence interval as derived from 50 bootstrap runs. The region between the purple horizontal lines represents chemostasis. Regions above and below it represent mobilization and dilution, respectively.

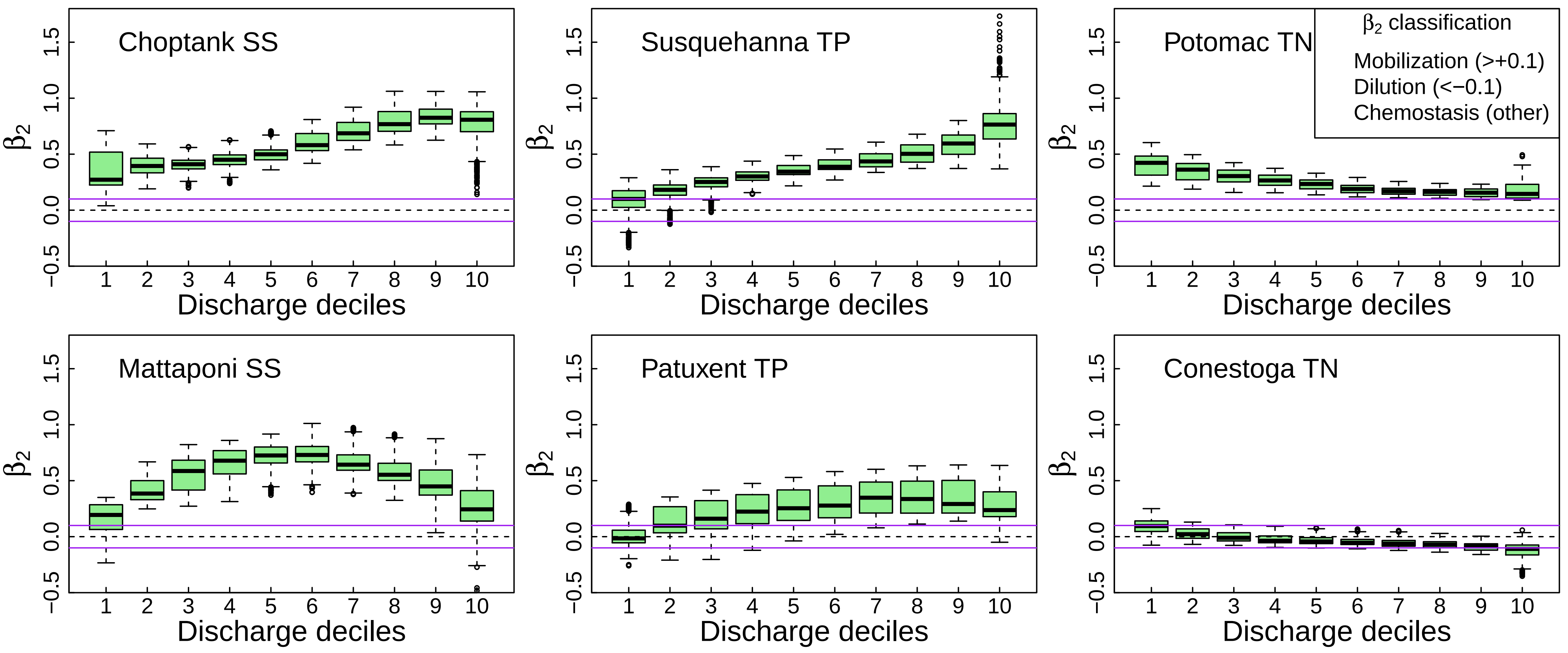
Choptank SS
Susquehanna TP
Potomac TN
Mattaponi SS
Patuxent TP
Conestoga TN
β_2 classification
Mobilization (>+0.1)
Dilution (<−0.1)
Chemostasis (other)
β_2
Discharge deciles